Synthesizing novel quantum/topological states of matter by periodic driving

AN Jun-Hong (安钧鸿)
Email: anjhong@lzu.edu.cn

Lanzhou University

@ CSRC Workshop on Quantum Non-Equilibrium Phenomena: Methods and Applications
Beijing, 2019年6月17日-21日

Outline

Outline

Outline

Phase transition

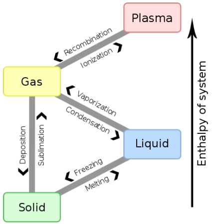

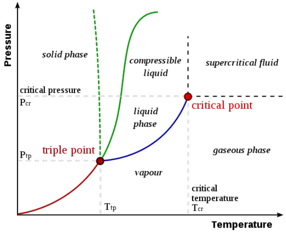

Phase transition (PT): System driven by control parameters changes from one state of matter to another

1. CPT: Abrupt change of $\mathcal{F}$ by changing T-relevant parameters
2. QPT: Abrupt change of E_g of a zero-T Q. many-body system

QPT

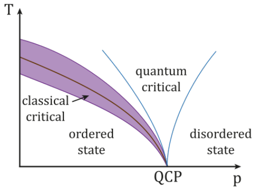

- Formation of novel order of collective mode
- Determined by energy spectrum: Abrupt opening of a bandgap
- Difficulty: The parameters are hard to change once the material sample of the system is fabricated

More efficient way to manipulate energy spectrum than changing parameters is desired

Periodic driving

- A useful tool in quantum control

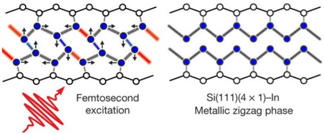

Optically excited structural transition in atomic wires. T. Frigge, et al., Nature 544, 207 (2017).

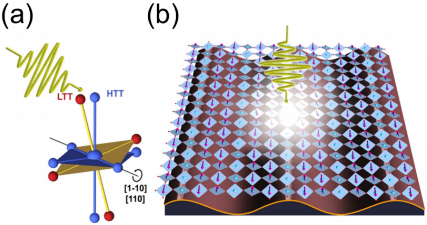

Light-induced high-Tc superconductivity. D. Fausti, et al., Science 331, 189 (2011)

offers high controllability to Q. system because time, as an extra dimension, is added to the system

Can we manipulate the energy spectrum by periodic driving?

DARPA program aims to extend lifetime of quantum systems (2018/01)

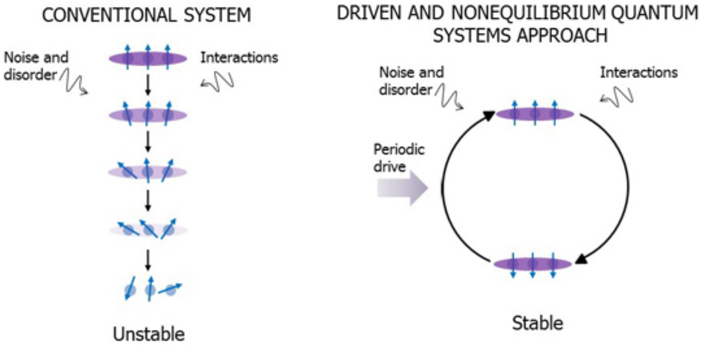

Time crystal

A many-body periodic system spontaneously self-organizes in time and starts evolving with a period that is not equal T?

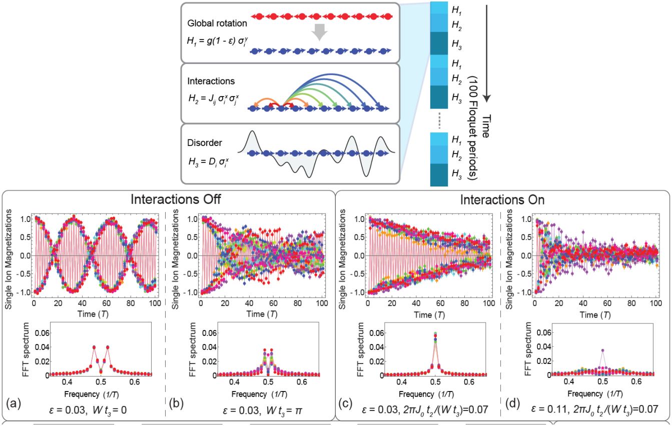

J. Zhang, et al., Nature 543, 217 (2017)

周期含时系统的Floquet定理

静态系统	周期性含时系统
$\hat{H}\lvert\varphi_n\rangle = E_n\lvert\varphi_n\rangle$	$[\hat{H}(t) - i\hbar\partial_t]\lvert\phi_n(t)\rangle = \varepsilon_n\lvert\phi_n(t)\rangle$ $\lvert\phi_n(t)\rangle = \lvert\phi_n(t+T)\rangle$
$\lvert\Psi(t)\rangle = \sum_n c_n e^{\frac{-iE_n t}{\hbar}}\lvert\varphi_n\rangle$ $c_n = \langle\varphi_n\lvert\Psi(0)\rangle$	$\lvert\Psi(t)\rangle = \sum_n c_n e^{\frac{-i\varepsilon_n t}{\hbar}}\lvert\phi_n(t)\rangle$ $c_n = \langle\phi_n(0)\lvert\Psi(0)\rangle$
E_n: 能谱 $\lvert\varphi_n\rangle$: 定态	ε_n: 准能谱Quasienergy $\lvert\phi_n(t)\rangle$: 准定态Quasi-stationary state

1. $e^{im\omega t}\lvert\phi_n(t)\rangle$ ($\omega = 2\pi/T$, $m \in \mathbb{Z}$) also the solution of Floquet equation with quasienergy $\varepsilon_n + m\hbar\omega$
2. The quasienergy is periodic. One generally chooses $[-\hbar\omega/2, \hbar\omega/2]$ called first Brillouin zone

Outline

1. Introduction
   - QPT & periodic driving
   - Quasienergy spectrum
   - Nonequilibrium QPT by periodic driving
   - Nonequilibrium TPT by periodic driving
2. Generating multiple MFs
   - Motivation
   - System and results
   - Summary
3. Synthesizing large-Chern-number TI
   - Motivation
   - System and results
   - Realization in cold atom system
   - Summary
4. Conclusions

Effective Hamiltonian

$$[\hat{H}(t) - i\hbar\partial_t]|\phi_n(t)\rangle = \varepsilon_n|\phi_n(t)\rangle$$
$$\hat{U}_T|\phi_n(0)\rangle = e^{\frac{-i}{\hbar}\varepsilon_n T}|\phi_n(0)\rangle$$

$$\hat{U}_T = \hat{\mathcal{T}}e^{-\frac{i}{\hbar}\int_0^T \hat{H}(t)dt} \equiv e^{\frac{-i}{\hbar}\hat{H}_{\text{eff}}T},\ \hat{H}_{\text{eff}}|\phi_n(0)\rangle = \varepsilon_n|\phi_n(0)\rangle$$

- An effective static system is defined
- The energy spectrum of $\hat{H}_{\text{eff}}$ is the same as the quasienergy spectrum of $\hat{H}(t)$

How to solve Floquet equation

$$\left.\begin{array}{c}[\hat{H}(t)-i\hbar\partial_t]|\phi_n(t)\rangle=\varepsilon_n|\phi_n(t)\rangle\\ |\phi_n(t)\rangle=\sum_{k\in\mathbb{Z}}e^{-ik\omega t}|\tilde{u}_n(k)\rangle\end{array}\right\}$$

$$\Rightarrow\sum_{k\in Z}[\hat{\tilde{H}}_{l-k}-k\omega\delta_{l,k}]|\tilde{u}_n(k)\rangle=\varepsilon_n|\tilde{u}_n(l)\rangle$$

with $\hat{\tilde{H}}_{l-k}=\frac{1}{T}\int_0^T\hat{H}(t)e^{i(l-k)\omega t}dt$. Thus

$$\begin{pmatrix}\ddots & \vdots & \vdots & \vdots & \iddots\\ \dots & \hat{\tilde{H}}_0+\hbar\omega & \hat{\tilde{H}}_{-1} & \hat{\tilde{H}}_{-2} & \dots\\ \dots & \hat{\tilde{H}}_1 & \hat{\tilde{H}}_0 & \hat{\tilde{H}}_{-1} & \dots\\ \dots & \hat{\tilde{H}}_2 & \hat{\tilde{H}}_1 & \hat{\tilde{H}}_0-\hbar\omega & \dots\\ \iddots & \vdots & \vdots & \vdots & \ddots\end{pmatrix}\begin{pmatrix}\vdots\\ |\tilde{u}_n(-1)\rangle\\ |\tilde{u}_n(0)\rangle\\ |\tilde{u}_n(1)\rangle\\ \vdots\end{pmatrix}=\varepsilon_n\begin{pmatrix}\vdots\\ |\tilde{u}_n(-1)\rangle\\ |\tilde{u}_n(0)\rangle\\ |\tilde{u}_n(1)\rangle\\ \vdots\end{pmatrix}\tag{1}$$

A periodically driven TLS

$$\begin{aligned}\hat{H}(t) &= \hat{H}_0 + \hat{H}_I(t) \\ \hat{H}_0 &= \frac{\hbar\omega_0}{2}\hat{\sigma}_z,\ \hat{H}_I(t) = \hbar A\cos(\omega t)\hat{\sigma}_x \end{aligned} \tag{2}$$

In the interaction picture,

$$\hat{H}_I^{(I)}(t) = \frac{\hbar A}{2}[\hat{\sigma}_+ e^{i(\omega_0+\omega)t} + \hat{\sigma}_+ e^{i(\omega_0-\omega)t} + \text{H.c.}]$$

- $A \ll \omega_0$: RWA: Neglect the rapidly oscillating term

$$\hat{H}_{\text{RWA}}(t) = \frac{\hbar\omega_0}{2}\hat{\sigma}_z + \frac{\hbar A}{2}(e^{-i\omega t}\hat{\sigma}_+ + \text{H.c.})$$

Quasienergy spectrum under RWA

$$[\hat{H}_{\text{RWA}}(t) - i\hbar\partial_t]|\phi_n(t)\rangle = \varepsilon_n|\phi_n(t)\rangle$$

$$\Rightarrow \begin{cases} [\hat{H}'(t) - i\hbar\partial_t]|\phi'_n(t)\rangle = \varepsilon_n|\phi'_n(t)\rangle \\ \hat{H}'(t) = \hat{G}_t[\hat{H}_{\text{RWA}}(t) - i\hbar\partial_t]\hat{G}_t^\dagger,\ |\phi'_n(t)\rangle = \hat{G}_t|\phi_n(t)\rangle \end{cases}$$

$\hat{G}_t = e^{i\omega t\hat{\sigma}_+\hat{\sigma}_-}$ makes $\hat{H}'(t) = \frac{\hbar\Delta}{2}\hat{\sigma}_z + \frac{\hbar A}{2}\hat{\sigma}_x - \frac{\hbar\omega}{2}$ t-independent. $\hat{\tilde{H}}_0 = \hat{H}'$, $\hat{\tilde{H}}_{k\neq 0} = 0$ in Eq. (1). Different BZs are decoupled. The solution in kth BZ is

$$\varepsilon_{k,1} = -(k+\frac{1}{2})\hbar\omega + \frac{\hbar\mu}{2}, |\tilde{u}'_1(k)\rangle = \sin\theta|g\rangle + \cos\theta|e\rangle \quad (3)$$

$$\varepsilon_{k,2} = -(k+\frac{1}{2})\hbar\omega - \frac{\hbar\mu}{2}, |\tilde{u}'_2(k)\rangle = \cos\theta|g\rangle - \sin\theta|e\rangle, \quad (4)$$

with $\Delta = \omega_0 - \omega$, $\mu = \sqrt{\Delta^2 + A^2}$ and $\tan 2\theta = A/\Delta$.

Thus

$$|\phi_1'(t)\rangle = \sum_{k\in\mathbb{Z}} e^{-ik\omega t}|\tilde{u}_1'(k)\rangle = \sin\theta|g\rangle + \cos\theta|e\rangle$$
$$|\phi_2'(t)\rangle = \sum_{k\in\mathbb{Z}} e^{-ik\omega t}|\tilde{u}_2'(k)\rangle = \cos\theta|g\rangle - \sin\theta|e\rangle$$

Then

$$|\phi_1(t)\rangle = \hat{G}_t^\dagger|\phi_1'(t)\rangle = \sin\theta|g\rangle + e^{-i\omega t}\cos\theta|e\rangle$$
$$|\phi_2(t)\rangle = \hat{G}_t^\dagger|\phi_1'(t)\rangle = \cos\theta|g\rangle - e^{-i\omega t}\sin\theta|e\rangle$$

Quasistationary states

One can prove $|\phi_j(t)\rangle$ are

- periodic with period T: $|\phi_j(t)\rangle = |\phi_j(t+T)\rangle$
- are quasistationary states

$$\begin{aligned} \hat{U}(t) &= \mathcal{T} e^{\frac{-i}{\hbar}\int_0^t \hat{H}_{\text{RWA}}(\tau)d\tau} = \hat{G}_t^\dagger e^{\frac{-i}{\hbar}\hat{H}' t} \\ &= \sum_{j=1,2} e^{\frac{-i\varepsilon_j t}{\hbar}} |\phi_j(t)\rangle\langle\phi_j(0)| \end{aligned} \tag{5}$$

Same as what is claimed by the Floquet theorem

Quasienergy spectrum beyond RWA

Using Eq. (2), we have the nonzero elements of Eq. (1)

$$\hat{\tilde{H}}_0 = \frac{\hbar\omega_0}{2}\hat{\sigma}_z, \tag{6}$$

$$\hat{\tilde{H}}_{\pm 1} = \frac{\hbar A}{2}\hat{\sigma}_x \tag{7}$$

The quasienergy spectrum can be obtained from Eq. (1)

- An infinite-rank matrix equation. Truncation vs convergent

Comparison

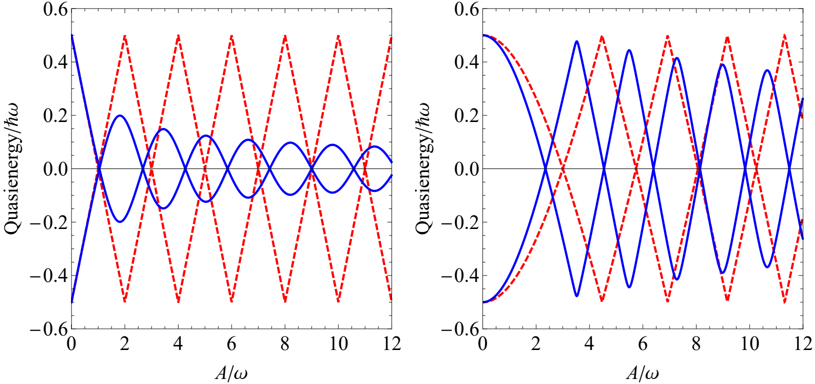

Comparision of the quasienergy spectrum of a periodically driven two-level system with (dashed red) and without RWA (solid blue) when $\omega_0 = \omega$ (left) and $\omega_0 = 5\omega$.

Coincide in the weak-driving and near-resonance regime

Exercise

Determine the quasienergy spectrum of

$$\hat{H}(t) = \hbar\omega_0 \hat{J}_z + \hbar f(t)\hat{J}_x, \tag{8}$$

with $\hat{\mathbf{J}}$ being angular momentum operator when

1. $f(t) = A\cos(\omega t)$.
2. $f(t) = \begin{cases} A_1, & t \in [nT, (n+\frac{1}{2})T] \\ A_2, & t \in [(n+\frac{1}{2})T, (n+1)T] \end{cases}, \quad n \in \mathbb{Z}.$
3. $f(t) = \sum_n \delta(t - nT)$ with $n \in \mathbb{Z}$.
4. $f(t) = \sum_n \delta(\frac{t}{T} - n)$ with $n \in \mathbb{Z}$.

Outline

Nonequilibrium QPT by periodic driving

is characterized by the abrupt opening of a bandgap in quasienergy spectrum by the driving parameters

- The energy is in non-conserving: Non-equilibrium
- A time-dependent analogy of QPT

The versatility of driving scheme enable us to

1. realize Q. phases not accessible for the static system in the same setting
2. explore novel Q. phases absent in the static system

A quick example

A periodically driven spin-1/2 particle interacting with a 1D spin chain Chen, **AN**, Luo, Sun, Oh, Phys. Rev. A 91, 052122 (2015)

$$
\begin{aligned}
\hat{H}_{\mathrm{S}}(t) &= \frac{1}{2}[\lambda + A(t)]\hat{\sigma}_0^z \\
\hat{H}_{\mathrm{I}} &= \frac{g}{2}(\hat{\sigma}_0^x\hat{\sigma}_1^x + \hat{\sigma}_0^y\hat{\sigma}_1^y) \\
\hat{H}_{\mathrm{E}} &= \frac{\lambda}{2}\sum_{j=1}^{L}\hat{\sigma}_j^z + \frac{J}{2}\sum_{j=1}^{L-1}(\hat{\sigma}_j^x\hat{\sigma}_{j+1}^x + \hat{\sigma}_j^y\hat{\sigma}_{j+1}^y)
\end{aligned}
$$

$$
A(t) = \begin{cases} a_1, & nT < t \leq nT + \tau \\ a_2, & nT + \tau < t \leq (n+1)T \end{cases}
$$

- Objective: Prevent the dissipation of system spin
- Initial state: $|\Psi(0)\rangle = |\uparrow_0\rangle \otimes |\{\downarrow_j\}\rangle$

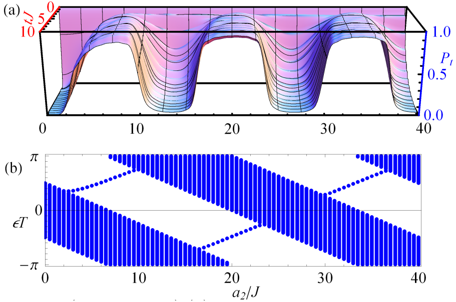

Evolution of $P_t = |c_0(t)|^2$ (a) and Floquet quasienergy spectrum of the whole system (b) in different driving amplitude a_2.

$$|\Psi(t)\rangle = e^{i\frac{L\lambda t}{2}}[xe^{-i\epsilon_{\text{FBS}}t}|\phi_{\text{FBS}}(t)\rangle + \sum_{\alpha\in\text{Band}} y_\alpha e^{-i\epsilon_\alpha t}|\phi_\alpha(t)\rangle],$$

The region where the dissipation is suppressed matches well with the one where a FBS is formed

Other driving conditions

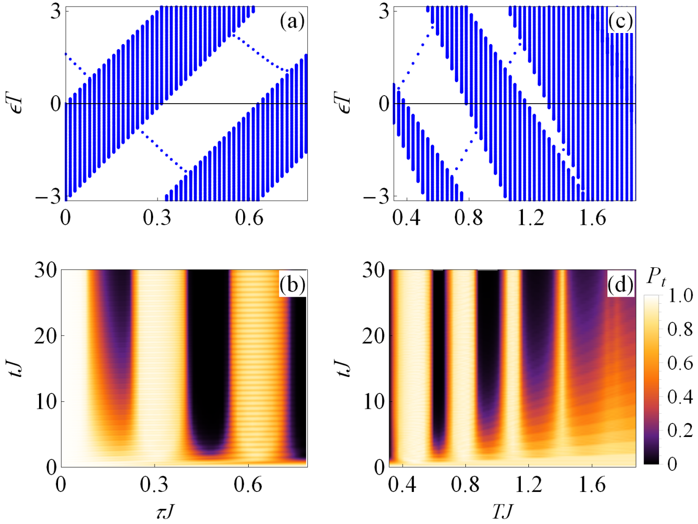

The Floquet spectrum (up) and the corresponding P_t (down) in different τ [(a) and (b)] when $T = 0.25\pi J^{-1}$ and in different T [(c) and (d)] when $\tau = 0.1\pi J^{-1}$.

Nonequilibrium phase diagram

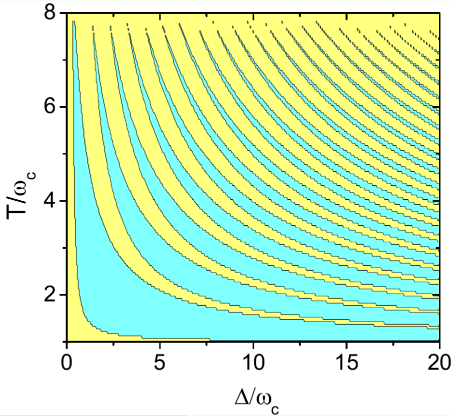

The non-equilibrium phase diagram of the driven system. The light yellow and cyan areas mean, respectively, the phases without and with the Floquet bound state. $\tau = 1.0\omega_c^{-1}$.

FBS $\Rightarrow$ Nonequilibrium QPT $\Rightarrow$ Decoherence suppression

Outline

Nonequilibrium TPT by periodic driving

Two-band model

$$\hat{H} = \sum_{\mathbf{k}\in BZ} \hat{C}_{\mathbf{k}}^{\dagger}\mathcal{H}(\mathbf{k})\hat{C}_{\mathbf{k}},\ \mathcal{H}(\mathbf{k}) = \varepsilon(\mathbf{k})I_{2\times 2} + \mathbf{h}(\mathbf{k})\cdot\boldsymbol{\sigma}$$

Driving protocol

$$\hat{H}(t) = \begin{cases} \hat{H}_1 = \hat{H}(\alpha,\beta),\ t\in[nT, nT+T_1] \\ \hat{H}_2 = \hat{H}(\alpha',\beta'),\ t\in[nT+T_1,(n+1)T] \end{cases}$$

with $T = T_1 + T_2$.

Xiong, Gong, **AN**, Phys. Rev. B 93, 184306 (2016)

Analytical results

Band touching condition $[\mathcal{H}_j(\mathbf{k}) = \epsilon_{\mathbf{k}} I_{2\times 2} + \mathbf{h}_j(\mathbf{k}) \cdot \boldsymbol{\sigma}]$

$$\mathbf{h}_1(\mathbf{k})/|\mathbf{h}_1(\mathbf{k})| = \pm \mathbf{h}_2(\mathbf{k})/|\mathbf{h}_2(\mathbf{k})|$$
$$T_1|\mathbf{h}_1(\mathbf{k})| \pm T_2|\mathbf{h}_2(\mathbf{k})| = n\pi, \; n \in \mathbb{Z}$$

1. It determines the phase transition boundaries
2. If n is even (odd), the band touches at quasienergy 0 ($\pm\pi/T$)
3. Connecting with the chirality of the Dirac points in the band-touching lines, $\Delta\mathcal{C}$ across the boundary is constant along the whole boundary

Outline

Outline

MF: Elementary particle

In 1937, Majorana: *Neutral spin-$\frac{1}{2}$ particle can be described by a real Dirac's equation, and thus is identical to its antiparticle*

- The particle at the matter-antimatter border
  - A particle of its own antiparticle: $\hat{\gamma}_A = (\hat{c}^\dagger + \hat{c})/2$, $\hat{\gamma}_B = (\hat{c}^\dagger - \hat{c})/2i \Rightarrow \hat{\gamma}_j = \hat{\gamma}_j^\dagger$

  - Non-abelian statistics
- Where is MF: No evidence. People suspect

Neutrino

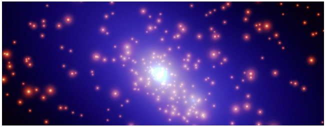

Dark matter

F. Wilczek, Nature Phys. 5, 614 (2009)

MF: Quasi-particle excitation in CMP

A superconductor system:

- Particle-hole symmetry: Its eigenmode is formed by the quasi-particle excitation:

$$\hat{\gamma}_E = \sum_{j=1}^{N} (u_{j,E} \hat{c}_j^\dagger + v_{j,E} \hat{c}_j)$$

  which may obey $\hat{\gamma}_{E=0} = \hat{\gamma}_{E=0}^\dagger$

- MF is simulated by a zero-energy quasi-excitation inside the vortex of a p-wave superconductor

  Ivanov, PRL 86, 268 (2001)

Schemes on realization

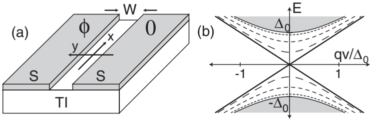

2D topological insulator. Fu and Kane, PRL 100, 096407 (2008)

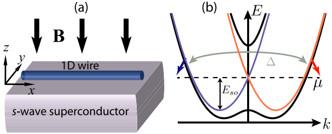

1D nanowire. (b): Time-reversal symmetry is present (red & blue) and broken by **B** (black). Lutchyn, Sau, and Das Sarma, PRL 105, 077001 (2010)

Conditions

1. Superconductor-topological insulator-superconductor structure
2. Majorana bound states at vortices

Conditions

1. Spin-orbit interactions in the nanowire
2. In the proximity to an s-wave superconductor
3. Moderate magnetic field

MF in QIS: Topological Q. computating

MFs define a topologically protected Q. memory

- 2 Majorana separated bound states = 1 fermion
  - 2 degenerate states (full/empty) = 1 qubit
- 2N separated Majoranas = N qubits
- Q. information is stored non locally
  - Immune from local decoherence
- Braiding performs unitary operations: Non-Abelian statistics

Ivanov, PRL 86, 268 (2001); Kitaev (2003)

Zero-bias peak of differential conductance as signature

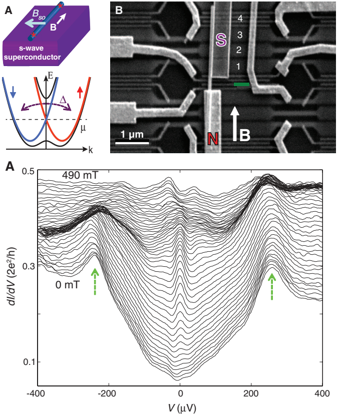

InSb nanowires contacted with one normal (gold) and one superconducting (NbTiN) electrode. Mourik *et al.*, Science 336, 1003 (2012)

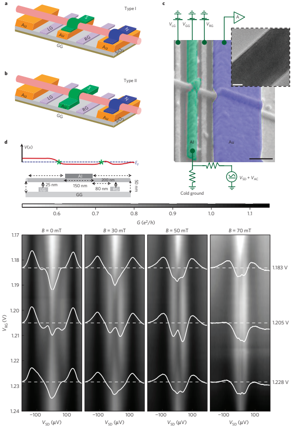

Al-InAs nanowire on gold pedestals above p-type silicon. Das, Ronen, Most, Oreg, Heiblum and Shtrikman, Nat. Phys. 8, 887 (2012)

Zero-bias peak of differential conductance

The zero-bias peak can also be generated in topologically trivial system due to

- the strong disorder in the nanowire

  Liu, Potter, Law, Lee, PRL 109, 267002 (2012)

  Pikulin, Dahlhaus, Wimmer, Schomerus, Beenakker, NJP 14, 125011 (2012)

- the smooth confinement potential at the wire end

  Kells, Meidan, Brouwer, PRB 86, 100503(R) (2012)

"... implies that the mere observation of a zero-bias peak in the tunneling conductance is not an exclusive signature of a topological superconducting phase"

More ways to double-confirm the formation of MF are desired

Motivation

1. Can periodic driving induce more MFs to enhance the experimental signal generated by MFs?
2. Can periodic driving supply a novel way to identify the experimental signal generated by MFs from other mechanism?

Outline

Model

$$\hat{H} = -\mu \sum_{l=1}^{N} \hat{c}_l^\dagger \hat{c}_l - \sum_{a=1}^{2} \sum_{l=1}^{N-a} (t_a \hat{c}_l^\dagger \hat{c}_{l+a} + \Delta_a \hat{c}_l^\dagger \hat{c}_{l+a}^\dagger + \text{H.c.})$$

- Chemical potential: μ
- Hopping amplitude: t_a
- Pairing potential: $\Delta_a = |\Delta_a| e^{i\phi_a}$

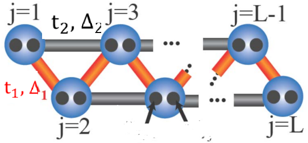

$\phi = \phi_1 - \phi_2$ determines the topological class [1]

	Symmetry	T. class	T. invariant	MMs[2]
$\phi = 0, \pi$	T,PH,C	BDI	$\mathbb{Z}$	2
$\phi =$other	PH	D	$\mathbb{Z}_2$	1

[1] Ryu, Schnyder, Furusaki, and Ludwig, NJP **12**, 065010 (2010)

[2] Schnyder, Ryu, Furusaki, and Ludwig, PRB **78**, 195125 (2008)

How to generate more MFs

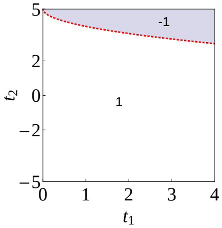

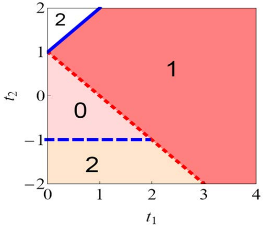

Phase diagram in D class charactarized by ν (left) and BDI class characterized by winding number W (right)

Two ingredients in generating more MFs [3]

1. Time reversal symmetry
2. Long-range interactions

Both introduce additional difficulties to the practical experiments

[3] Niu, Chung, Hsu, Mandal, Raghu, and Chakravarty, PRB **85**, 035110 (2012)

Driving protocol

$$\hat{H}(t) = \begin{cases} \hat{H}_1 = \hat{H}(\phi_1, \phi_2), & \text{if } \; t \in [nT, (n+1/2)T) \\ \hat{H}_2 = \hat{H}(\phi_2, \phi_1), & \text{if } \; t \in [(n+1/2)T, (n+1)T) \end{cases}$$

- For $\hat{H}_1$ and $\hat{H}_2$, the system is in D class, where at most one pair of MFs can be formed

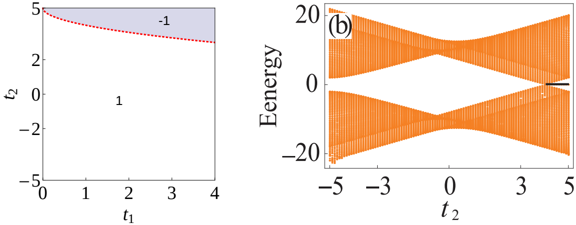

Phase diagram in D class characterized by ν (left) and the corresponding energy spectrum

Role of periodic driving in $\hat{H}_{\text{eff}}$

$$\hat{U}_T|\phi_n(0)\rangle = e^{\frac{-i}{\hbar}\hat{H}_{\text{eff}}T}|\phi_n(0)\rangle$$

Tong, An, Gong, Luo, Oh, Phys. Rev. B 87, 201109(R) (2013)

1. Restore time-reversal symmetry

$$\hat{\hat{\mathcal{K}}}\hat{U}_T\hat{\hat{\mathcal{K}}}^{-1} = e^{\frac{i\hat{H}_1T}{2\hbar}}e^{\frac{i\hat{H}_2T}{2\hbar}} = \hat{U}_T^\dagger,$$

with $\hat{\hat{\mathcal{K}}} \equiv \hat{\mathcal{K}}\hat{G}$ and $\hat{G} = e^{-i\frac{\phi_1+\phi_2}{2}\sum_l c_l^\dagger c_l}$.

2. Synthesize longer-range interaction (Baker-Campbell-Hausdorff formula)

$$\hat{U}_T = e^{-\frac{iT}{2\hbar}\hat{H}_2}e^{-\frac{iT}{2\hbar}\hat{H}_1} \equiv e^{\frac{-i}{\hbar}\hat{H}_{\text{eff}}T}$$
$$\hat{H}_{\text{eff}} = \frac{\hat{H}_1+\hat{H}_2}{2} - \frac{iT}{8\hbar}[\hat{H}_2,\hat{H}_1] - \frac{T^2}{96\hbar^2}[\hat{H}_2-\hat{H}_1,[\hat{H}_2,\hat{H}_1]] + \cdots$$

Numerical confirmation

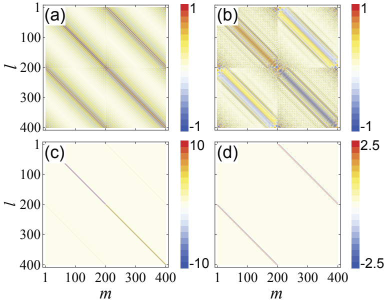

coefficients of Hamiltonian expanded in the operator basis $(c_1, \cdots, c_N, c_1^\dagger, \cdots, c_N^\dagger)^T$ when $T = 0.2$ (a) and 2.0 (b) and the real (c) and the imaginary (d) of static case.

1. Interaction range is enhanced for the driven case (a,b) comparing with the static case (c,d)
2. The expansion coefficients of $\hat{H}_{\text{eff}}$ are real, which confirms the restoring of time-reversal symmetry

Multiple MFs

1. Multiple MFs can be generated

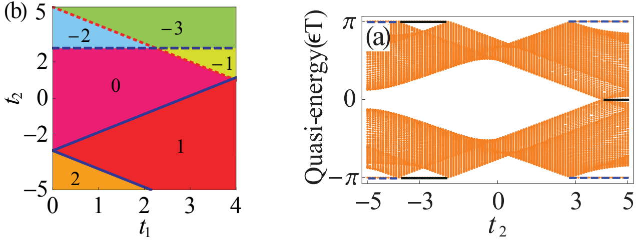

Phase diagram and quasi-energy spectrum of the periodically driven system. $T = 0.2$

2. We may go further by increasing T, which induces longer-range interactions in $\hat{H}_{\text{eff}}$

t_2	−8	−7	−6	−5	−4	−3	−2	−1	0	1	2	3	4	5	6	7	8
$T = 0.5$	2	4	4	3	3	2	0	0	0	1	1	2	2	4	4	4	3
$T = 1.0$	6	6	7	7	6	3	3	2	1	1	2	5	5	6	7	7	6
$T = 2.0$	13	13	12	11	9	8	8	1	1	3	4	7	11	10	13	13	12

Spatial distribution of MFs

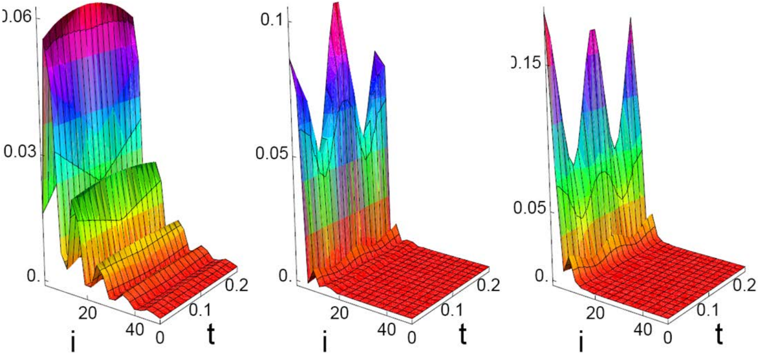

The evolution of the distribution of the generated three MFs over the lattices

All the generated MFs are confined in the lattice edge during time evolution

Outline

Summary

- The number of the MFs may be greatly enhanced and widely tuned by periodic driving
  1. The enhanced signal is more robust against experimental disorder and contaminations from thermal excitations
  2. It supplies a novel way to identify if the signal originates from MFs by observing the change of the signal in response of the tuning of the driving coefficients
- The generation of a tunable number of MFs is expected to offer another dimension for experimental studies

Outline

Outline

Topological insulator

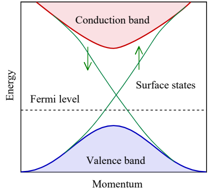

- has a bulk energy gap like an ordinary insulator
- has gapless states localized spatially at the surface/edge like a conductor
- is related to quantum Hall effect on the edge states
- can be characterized by topological invariant: Winding number, Chern number, Z_2

新奇拓扑物态

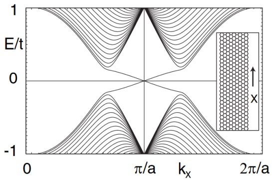

量子自旋霍尔效应 (Kane, Mele, 2005)

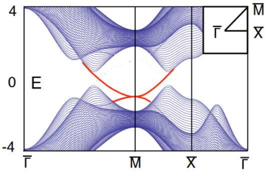

拓扑晶体绝缘体 (Liang Fu, 2011)

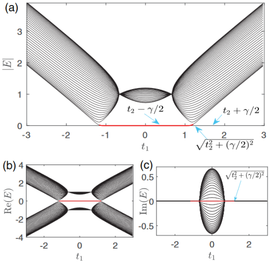

非厄米拓扑物态 (Zhong Wang, 2018)

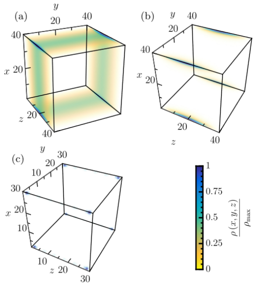

高阶拓扑物态 (Bitan Roy, 2019)

TI with large Chern number

TI with large Chern number

- with higher plateau QAH effect would lead to novel designs for low power-consumption electronics J. Wang, B. Lian, H. Zhang, Y. Xu, and S.-C. Zhang, PRL 111, 136801 (2013)
- could improve the performance of the interconnect devices by lowering the contact resistance C. Fang, M. J. Gilbert, and B A. Bernevig, PRL 112, 046801 (2014)
- plays a key role of realizing new photonic devices S. A. Skirlo, L. Lu, Y. Igarashi, J. Joannopoulos, and M. Soljacic, PRL 115, 253901 (2015); S. A. Skirlo, L, Lu, and M. Soljačić, PRL 113, 113904 (2014)

Generate TI with large Chern number

- Long-range interactions

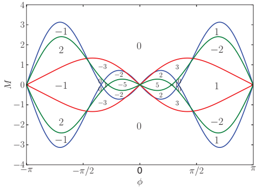

Haldane model with 6^{th}-order hopping. D. Sticlet and F. Piéchon, Phys. Rev. B 87, 115402 (2013)

- Multilayer materials

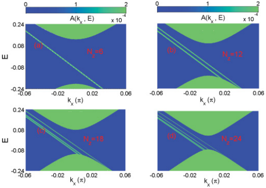

Dispersion relation with laymer thickness. H. Jiang, Z. Qiao, H. Liu, and Q. Niu, Phys. Rev. B 85, 045445 (2012)

Experiments

- Only $|C| = 1$ for electronic system is observed C.-Z. Chang, et al., Science 340, 167 (2013); G. Jotzu, et al., Nature 515, 237 (2014)
- Up to $|C| = 4$ is observed in microwave simulation in photonic crystal

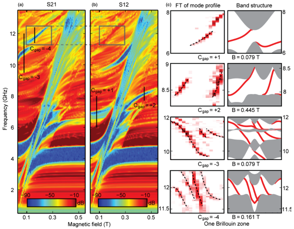

S. A. Skirlo, L. Lu, Y. Igarashi, J. Joannopoulos, and M. Soljacic, PRL 115, 253901 (2015)

Do we have more efficient way to engineer large-Chern-number topological phases?

Photonic Floquet TI

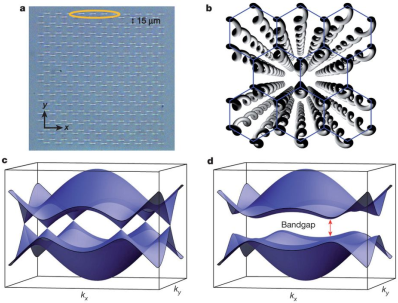

M. C. Rechtsman, et al., Nature 496, 196 (2013)

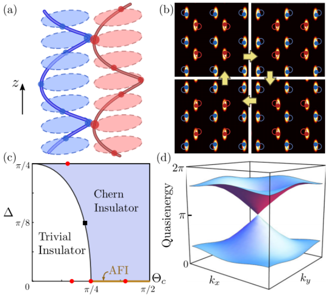

D. Leykam, et al., PRL 117, 013902 (2016)

The formal similarity of Schrödinger equation governing the temporal evolution of a wave packet to the spatial propagation of a light beam in the paraxial approximation

Outline

Periodically driven Haldane model

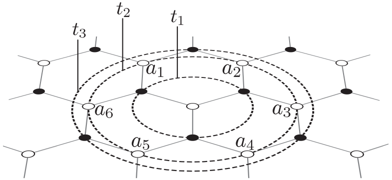

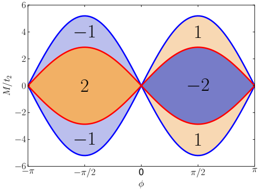

3[rd] hopping Haldane model and its static PD. D. Sticlet and F. Piéchon, Phys. Rev. B 87, 115402 (2013)

- Nonequilibrium PD $H_1 = H(t_3 = \frac{3t_1}{4}, \phi = \frac{-\pi}{6})$, $H_2 = H(t_3 = \frac{-3t_1}{4}, \phi = \frac{-\pi}{2})$

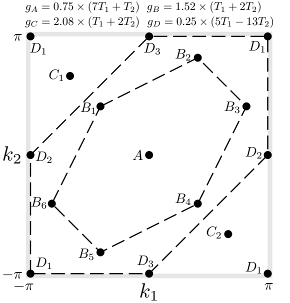

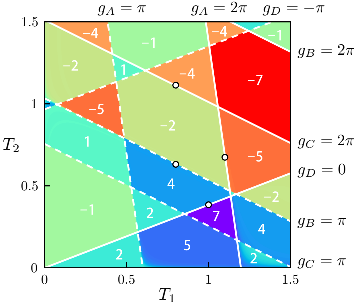

Xiong, Gong, **AN**, Phys. Rev. B 93, 184306 (2016)

- Dirac cones at phase border

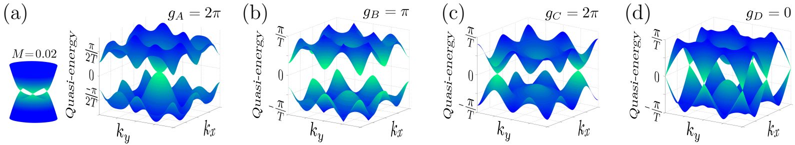

- Quasienergy spectrum

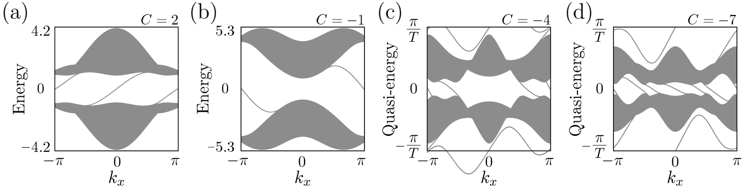

Energy spectrum for static H_1(a) and H_2(b); Qasienergy spectrum under periodic driving $(T_1, T_2) = (0.9, 1.2)$(c) and $(T_1, T_2) = (1.3, 1.2)$(d).

Time evolution of the edge modes

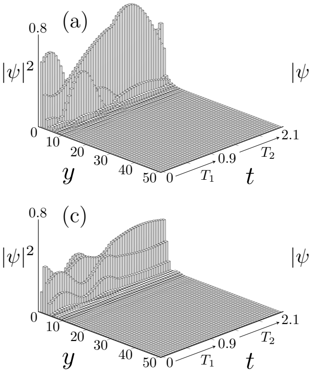

All the four edge states are confined at the edge during time evolution

Outline

Spin-orbit coupling in 1D cold atom

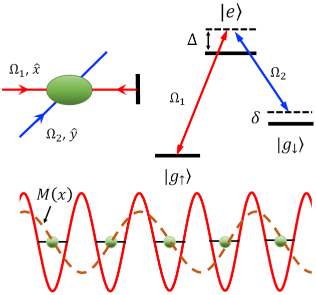

X.-J. Liu, Z.-X. Liu, and M. Cheng, Phys. Rev. Lett. 110, 076401 (2013)

A standing wave (red):
$V_{\text{ol}} = V_0 \cos^2 k_0 x$ with
$V_0 = |\Omega_1|^2/\Delta$
Further with the running wave (blue):
$M(x) = M_0 \cos k_0 x$ with
$M_0 = |\Omega_1 \Omega_2|/\Delta$

$$\hat{H} = \sum_\sigma \int dx \hat{\psi}_\sigma^\dagger(x)[\frac{p_x^2}{2m} + V_{ol}\cos^2(k_0 x) + \xi_\sigma m_z]\hat{\psi}_\sigma(x)$$

$$+M_0[\int dx \hat{\psi}_\uparrow^\dagger(x)\cos(k_0 x)\hat{\psi}_\downarrow(x) + \text{H.c.}]$$

Tight-binding Hamiltonian

If $M_0 \ll V_{\text{ol}}$: neglect interband spin-dependent coupling of the different orbital bands

$$\begin{aligned}
\hat{H} &= -\sum_{\langle i,j\rangle,\sigma} \lambda_{\text{s}}(i,j)\hat{\psi}^{\dagger}_{i\sigma}\hat{\psi}_{j\sigma} + m_z \sum_{i,\sigma} \xi_\sigma \hat{\psi}^{\dagger}_{i\sigma}\hat{\psi}_{i\sigma} \\
&\quad + \sum_{\langle i,j\rangle} [\lambda_{so}(i,j)\hat{\psi}^{\dagger}_{i\uparrow}\hat{\psi}_{j\downarrow} + \text{H.c.}], \\
v_0(i,j) &= \int dx \phi_i^*(x)[\frac{\hat{p}_x^2}{2m} + V_{ol}\cos^2(k_0 x)]\phi_j(x), \\
v_{so}(i,j) &= M_0 \int dx \phi_i^*(x)\cos(k_0 x + \varphi)\phi_j(x),
\end{aligned}$$

$\phi_j(x)$: the lowest band Wannier function on the jth site

Bogoliubov-de Gennes Hamiltonian

$\hat{H} = \sum_{k\in\mathrm{BZ}} \mathbf{C}_k^\dagger \mathcal{H}(k)\mathbf{C}_k$ with $\mathbf{C}_k^\dagger = (\hat{\psi}_{k\uparrow}^\dagger\ \hat{\psi}_{k\downarrow}^\dagger)$,
$\mathcal{H}(k) = \mathbf{h}(k)\cdot\boldsymbol{\sigma}$ and the Bloch vector

$$\mathbf{h}(k) = (0, 2v_{so}\sin k, m_z - 2v_0\cos k), \tag{9}$$

- Time-reversal symmetry: BDI class
- Topological invariant $\mathcal{W}$

$$\mathcal{W} = \begin{cases} 0, & \text{else} \\ \pm 1, & |m_z| \le 2|\lambda_s| \;\&\; \lambda_{so} \neq 0 \end{cases}$$

- At most one pair of edge state can be formed

Driving scheme

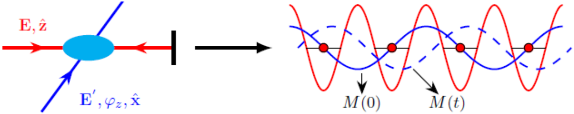

$$v_{so}(t) = \begin{cases} A_1, & t \in [mT, mT + T_1) \\ A_2, & t \in [mT + T_1, (m+1)T), \end{cases} \quad m \in \mathbb{Z},$$

which can be realized by periodically changing the driving strength M_0 of the Raman transition.

Liu, Xiong, Zhang, and **AN**, arXiv:1904.01950

Numerical results

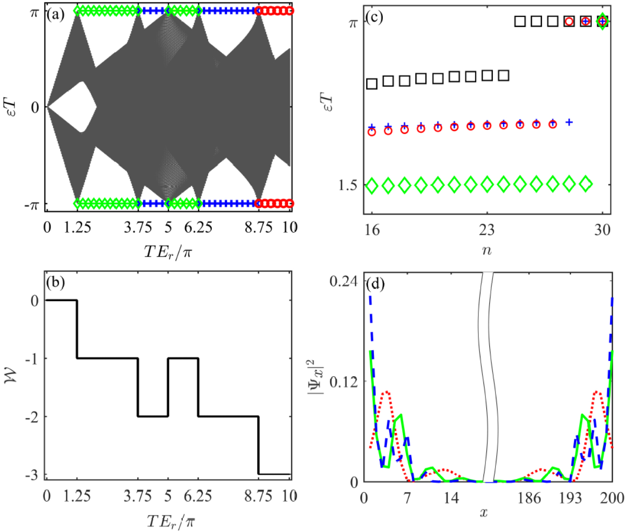

$E_r = \hbar^2 k_0^2/2m$ is the unit energy scale. $T_1 = T_2 = T/2$.

Numerical results: Phase diagram

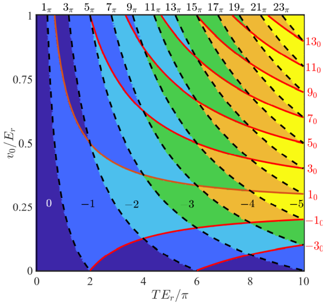

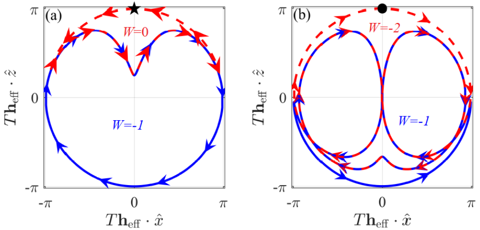

- PT condition: $n_\alpha = T|m_z - 2e^{i\alpha}v_0|/\pi$ for $\alpha = 0, \pi$
- $\mathcal{W}$ decreases (increases) 1 when T increases across the boundary caused by $k = \pi$ (0)

2D: Static case

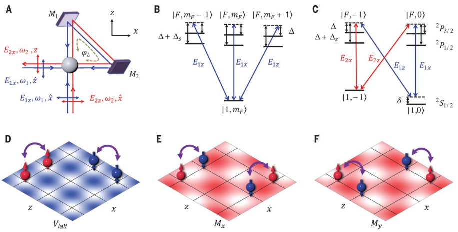

A recent realization. Z. Wu et al., Science 354, 83 (2016)

$$\mathbf{h}_{2D}(\mathbf{k}) = [2v_{so}\sin k_z, 2v_{so}\sin k_x, m_z - 2v_0(\cos k_x + \cos k_z)]$$

The Chern number

$$\mathcal{C} = \begin{cases} 0, & \text{else} \\ \text{sgn}(m_z), & |m_z| < 4|v_0| \end{cases}$$

At most one pair of edge states can be formed

2D: Periodic-driving case

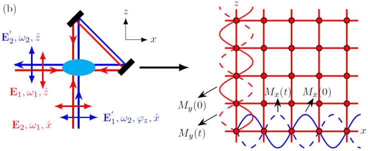

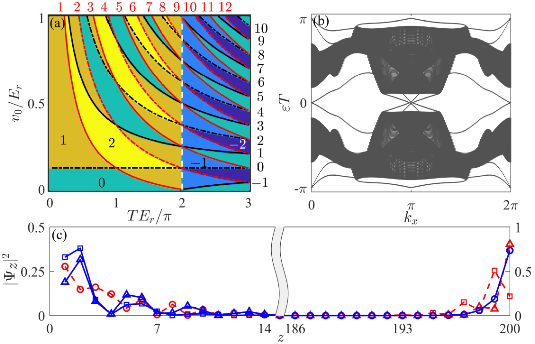

The blue solid (red dashed) lines marked by △, □ and ○ are the zero (π/T) modes.

- PT condition: $T|m_z - 2(e^{i\alpha} + e^{i\beta})v_0| = n\pi$ with $\alpha, \beta = 0$ or π
- Breakdown of bulk-edge correspondence
- $|\mathcal{C}| = 2$ at most, but many edge states are formed

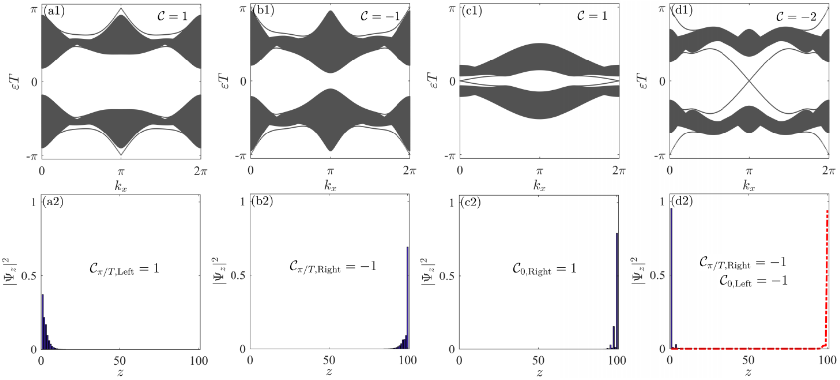

- Bulk-edge correspondence is recovered by considering the respective contribution of two types of edge states

Outline

Summary

- Nonequilirium topological insulator phases can be triggered by periodic driving
- It can be used to artificially synthesize extremal topological states of matter absent in its static correspondence

Outline

Conclusions

- We may manipulate (quasi)energy spectrum by periodic driving such that exotic QPT/TPT is triggered
- Periodically driven system may exhibit novel properties absent in its static correspondence

Outlook: Weyl semimetal

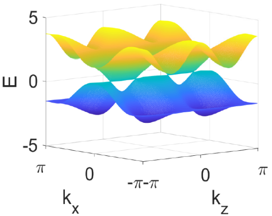

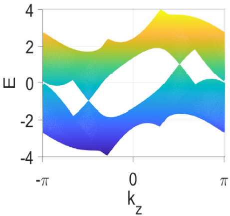

Periodic-driving-induced III-type semimetal (L), I- and II-type coexistence (R)

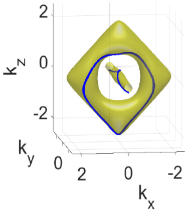

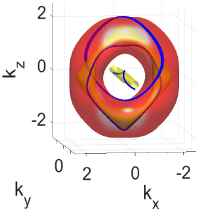

Periodic-driving-induced exotic topological nodal line semimetals

Wu, **AN**, in preparation

Thank you for your attention!

Decoherence in noisy quantum metrology

AN Jun-Hong (安钧鸿)
Email: anjhong@lzu.edu.cn

Lanzhou University

@ CSRC Workshop on Quantum Non-Equilibrium Phenomena: Methods and Applications
Beijing, 2019年6月17日-21日

Contents

Contents

Contents

Metrology

- Metrology: Develop methods to measure physical quantities in high precision
  - Define international units of measurement
  - Realize these units of measurement in practice
- Measurement errors VS repeating measurements

$$\begin{aligned}\delta x &= \Delta\sigma/\sqrt{M} \quad \text{Central limit theorem}\\ &\geq 1/\sqrt{MF(x)} \quad \text{Cramér-Rao bound}\end{aligned}$$

  - M: Measurement times
  - $\Delta\sigma$: Standard deviation
  - $F(x) = \sum_{i=1}^{M} [\partial_x p_i(x)]^2 / p_i(x)$: Fisher information; $p_i(x)$: Measured probability distribution of x

Q. metrology

- Q. metrology employs Q. effects to attain a precision surpassing the limit achievable in classical physics
  - Q. squeezing
  - Q. entanglement
- It has profound impact on
  - Q. lidar/radar (positioning)
  - Atomic clock (frequency)
  - Q. magnetometer (magnetism)
  - Q. imaging (photography)
  - Q. gyroscope (navigation)

A great technique innovation triggered by Q. theory

Mach-Zehnder interferometer

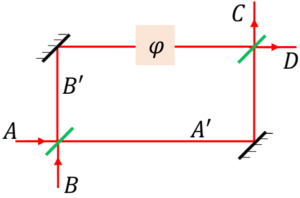

Mach-Zehnder interferometer

$\hat{V} = \exp[i\frac{\pi}{4}(\hat{a}_A^\dagger \hat{a}_B + \hat{a}_B^\dagger \hat{a}_A)]$: 50:50 beam splitter
$\hat{U} = \exp[i\varphi \hat{a}_B^\dagger \hat{a}_B]$: Phase shift to encode

- Input-output relation

$$|\psi_{\text{out}}\rangle = \hat{V}\hat{U}\hat{V}|\psi_{\text{in}}\rangle$$

- Measure $\bar{O} = \langle\psi_{\text{out}}|\hat{O}|\psi_{\text{out}}\rangle$, $\delta O = \sqrt{\overline{O^2} - \bar{O}^2}$
- Parameter estimation

$$\delta\varphi = \frac{\delta O}{|\partial\bar{O}/\partial\varphi|}$$

$\hat{O} = \hat{a}_A^\dagger \hat{a}_A - \hat{a}_B^\dagger \hat{a}_B$

- Coherent state $|\psi_{\text{in}}\rangle = |\alpha_A, 0_B\rangle$ ($\bar{n} = |\alpha|^2$):

$$\min \delta\varphi = 1/\sqrt{\bar{n}} \quad \text{Standard Q. limit (SQL)}$$

- Squeezed state $|\psi_{\text{in}}\rangle = |\alpha_A, \xi_B\rangle$ ($\xi = re^{i\phi}$):

$$\min \delta\varphi = e^{-r}/\sqrt{\bar{n}} \simeq \frac{1}{N^{3/4}} \quad \text{Zeno limit (ZL)}$$

- Entangled state $|\psi_{\text{in}}\rangle = \frac{1}{\sqrt{2}}(|n_A^+, n_B^-\rangle + |n_A^-, n_B^+\rangle)$ ($n^\pm = \frac{n\pm 1}{2}$):

$$\min \delta\varphi = 1/n \quad \text{Heisenberg limit (HL)}$$

V. Giovannetti, S. Lloyd, and L. Maccone, Science 306, 1330 (2004)

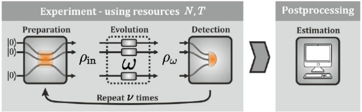

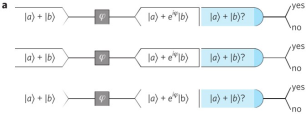

R. Chaves, *et al.*, PRL 111, 120401 (2013)

Uncorrelated input state

1. Input: $|g\rangle^{\otimes N} \xrightarrow{\pi/2 \text{ pulse}} [(|g\rangle + |e\rangle)/\sqrt{2}]^{\otimes N}$
2. Encode: $\xrightarrow{\text{Free evolution}} [(e^{\frac{i\omega_0 t}{2}}|g\rangle + e^{\frac{-i\omega_0 t}{2}}|e\rangle)/\sqrt{2}]^{\otimes N}$
3. Detect: $\xrightarrow{\pi/2 \text{ pulse}} [\cos\frac{\omega_0 t}{2}|g\rangle + i\sin\frac{\omega_0 t}{2}|e\rangle]^{\otimes N}$

$$\xrightarrow{\text{Measure } \hat{O} = \hat{\sigma}_+\hat{\sigma}_-} \bar{O} = \sin^2\frac{\omega_0 t}{2}, \ \Delta O = |\sin\omega_0 t|/2$$

4. Repeating detection in T: We obtain $M = NT/t$ copies of measurement results

$$\delta O = \sqrt{\frac{\Delta O}{M}} = \sqrt{\frac{|\sin \omega_0 t|}{2NT/t}}$$

5. Estimate:

$$\delta\omega_0 = \frac{\delta O}{|d\bar{O}/d\omega_0|} = (NTt)^{-1/2} \quad \text{SQL}$$

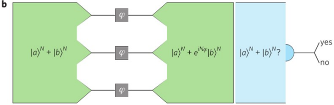

Entangled input state

1. Input: $|g\rangle^{\otimes N} \xrightarrow{\pi/2 \text{ pulse}} \frac{|g\rangle + |e\rangle}{\sqrt{2}} \otimes |g\rangle^{\otimes N-1}$
$\xrightarrow{\text{CNOT}} (|g\rangle^{\otimes N} + |e\rangle^{\otimes N})/\sqrt{2}$
2. Encode: $\xrightarrow{\text{Free evolution}} (e^{\frac{iN\omega_0 t}{2}}|g\rangle^{\otimes N} + e^{\frac{-iN\omega_0 t}{2}}|e\rangle^{\otimes N})/\sqrt{2}$
3. Detect:

$$\xrightarrow{\text{CNOT}} \frac{e^{\frac{iN\omega_0 t}{2}}|g\rangle + e^{\frac{-iN\omega_0 t}{2}}|e\rangle}{\sqrt{2}} \otimes |g\rangle^{\otimes N-1}$$

$$\xrightarrow{\pi/2 \text{ pulse}} [\cos\frac{N\omega_0 t}{2}|g\rangle + i\sin\frac{N\omega_0 t}{2}|e\rangle] \otimes |g\rangle^{\otimes N-1}$$

$$\xrightarrow{\text{Measure } \hat{O} = \hat{\sigma}_+\hat{\sigma}_-} \bar{O} = \sin^2\frac{N\omega_0 t}{2},\ \Delta O = |\sin N\omega_0 t|/2$$

4. Repeating detection in T: We obtain $M = T/t$ copies of measurement results

$$\delta O = \sqrt{\frac{\Delta O}{M}} = \sqrt{\frac{|\sin N\omega_0 t|}{2T/t}}$$

5. Estimation:

$$\delta\omega_0 = \frac{\delta O}{|d\bar{O}/d\omega_0|} = (N^2 Tt)^{-1/2} \quad \text{HL}$$

S. F. Huelga, *et al.*, PRL 79, 3865 (1997)

Application of Q. metrology

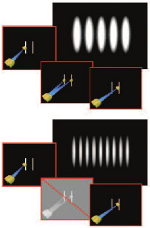

Q. lithography. P. Kok, S. L. Braunstein, J. P. Dowling (2002)

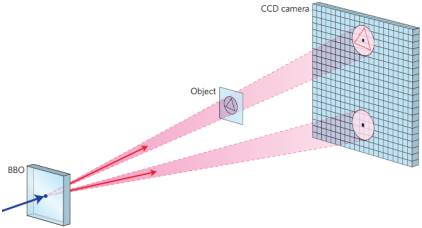

Q. imaging. G. Brida, M. Genovese, I. Ruo Berchera, Nat. Photon. 4, 227 (2010)

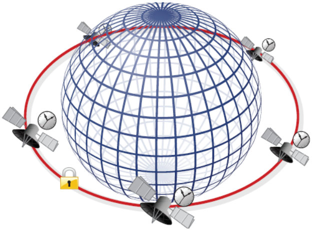

Entangled atomic clock. M. D. Lukin's group, Nat. Phys. 10, 582 (2014)

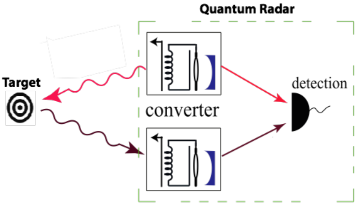

Q. radar. S. Barzanjeh et al., Phys. Rev. Lett. 114, 080503(2015)

Q. magnetometer

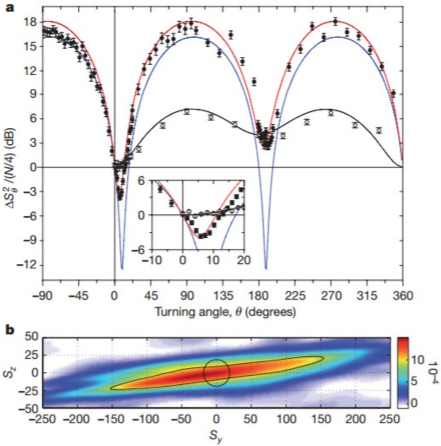

Spin squeezing. M. F. Riedel, et al., Nature 464, 1170 (2010)

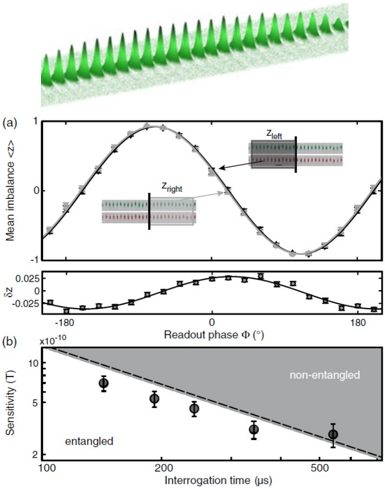

BEC自旋压缩导致的磁力计计量精度超越标准量子极限. W. Muessel, et al., PRL 113, 103004 (2014)

Squeezing-enhanced sensitivity

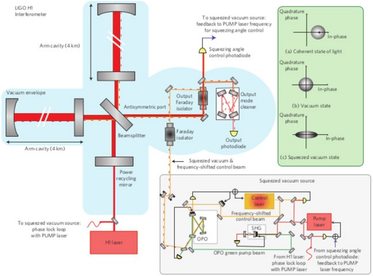

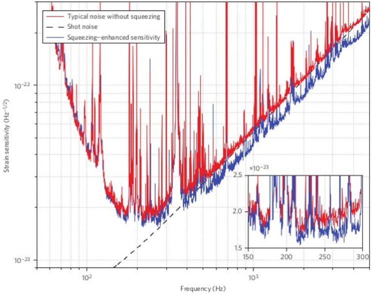

The LIGO Scientific Collaboration, Nature Photonics 7, 613 (2013)

Research focus in Q. metrology

- Given Q. resource, what is the ultimate limit of the precision: Q. Fisher information
  - Pure state $|\Psi(x)\rangle$:
    $\mathcal{F}_Q(x) = 4[\frac{d\langle\Psi(x)|}{dx}\frac{d|\Psi(x)\rangle}{dx} - |\frac{d\langle\Psi(x)|}{dx}|\Psi(x)\rangle|^2]$
  - Mixed state $\rho = \sum_i \lambda_i |\psi_i(x)\rangle\langle\psi_i(x)|$

$$
\begin{aligned}
\mathcal{F}_Q(x) &= \sum_i \left[\frac{1}{\lambda_i}\left(\frac{d\lambda_i}{dx}\right)^2 + \lambda_i \mathcal{F}_{Q,i}(x)\right] \\
&\quad -8\sum_{i\neq j}\frac{\lambda_i\lambda_j}{\lambda_i+\lambda_j}\left|\frac{d\langle\psi_i(x)|}{dx}|\psi_j(x)\rangle\right|^2
\end{aligned}
$$

Zhang, Li, Yang, Jin, 88, 043832 (2013)

- What measurement scheme can realize the ultimate limit
- How to evaluate and control decoherence effect

Contents

Decoherence

- The loss of coherence or of the phase ordering of the components of a Q. superposition
- The reason why Q. behaviors are different from classical one

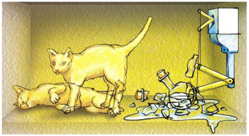

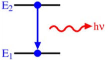

$|\Psi\rangle \rightarrow |00\cdots 0\rangle$

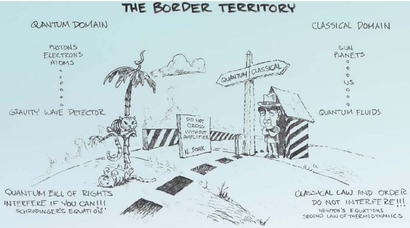

From W. H. Zurek (1991)

1. The border between Q. and classical world
2. Quantum-classical transition
3. The paradoxes when Q. laws are applied to macroscopic systems

Renewed interest in Q. engineering

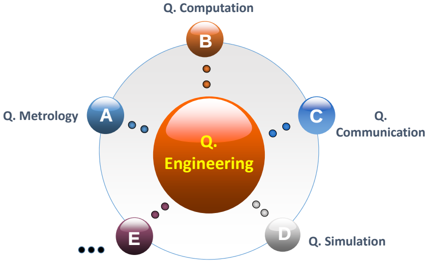

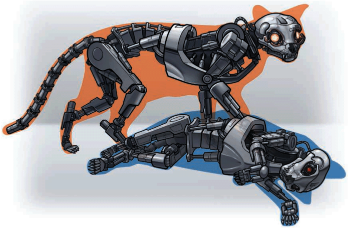

Mechanical analog to Schrödinger's cat. From Cho, Science 327 516 (2010).

- Great technique innovations from physical principle
- The realization of QE is bounded by decoherence

How to understand and control decoherence is crucial

Description of decoherence

Main idea

Tracing over the env. DoF from the unitary dynamics of the whole system consisting of the system and its env., the dynamics of the system is obtained.

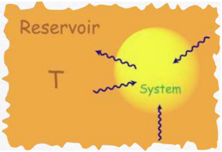

- Markovian vs non-Markovian: Coupling strength
- Dephasing vs dissipation: Energy exchange

Born-Markovian dynamics. Env. acts as a sink so that the energy flows irreversibly from the system to the env..

Non-Markovian dynamics. Env. coherently interplays with the system: dynamical backaction

Local Markovian dephasing noises

Ramsey interferometer: the atomic free evolution in encoding step is obscured by Q. noises

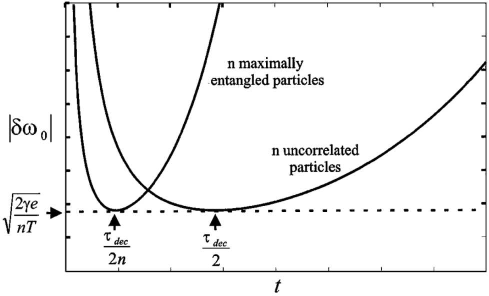

$$\delta\omega_0|_{\text{ent}} = \delta\omega_0|_{\text{unc}}$$

Q. advantage disappears completely

S. F. Huelga, *et al.*, PRL 79, 3865 (1997)

Local non-Markovian dephasing noises

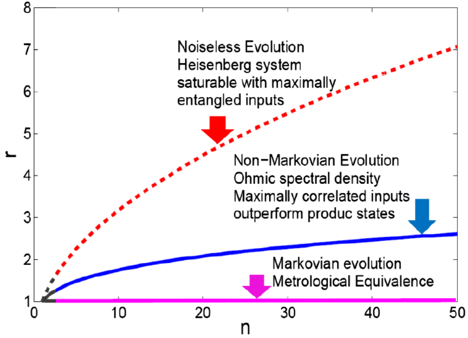

$$r = \delta\omega_0|_{\mathrm{unc}} / \delta\omega_0|_{\mathrm{ent}}$$

$$\delta\omega_0|_{\mathrm{ent}} \propto n^{-3/4} \quad \mathrm{ZL}$$

surpasses the SQL but does not achieve the HL

A. W. Chin, S. F. Huelga, and M. B. Plenio, PRL 109, 233601 (2012)

More on non-Markovian noises

In short-time Zeno dynamics, the ZL is obtainable

- for all local non-Markovian dephasing models K.

  Macieszczak, PRA 92, 010102(R) (2015)

- for all local phase-covariant noises in non-semigroup evolution A. Smirne, *et al.*, PRL 116, 120801 (2016)

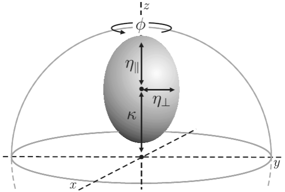

Phase covariant noise:
$[\Lambda_{\omega_0}(t), e^{-i\omega_0 t\sigma_z/2}] = 0$ with $\rho_{\omega_0}(t) = \Lambda_{\omega_0}(t)^{\otimes N}[\rho(0)]$

In long-time dynamics, $\delta\omega_0|_{\text{ent}} = \delta\omega_0|_{\text{unc}}$

Contents

Motivation

- Non-Markovian effect is helpful in improving metrology precision in noise case
- Can this helpful role performs better than achieving ZL?
- Is ideal precision achievable in noisy Q. metrology?
- How is the situation in dissipative noises?
  - Reason of atomic spontaneous emission
  - Main decoherence source in Ramsey and MZ interferometers

Contents

Contents

Local dissipative noises

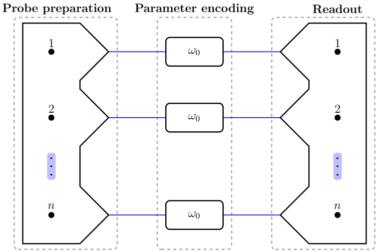

Ramsey interferometer to precisely estimating atomic frequency ω_0

Hamiltonian:

$$\hat{H}_j = \omega_0 \hat{\sigma}_j^+ \hat{\sigma}_j^- + \sum_k [\omega_k \hat{a}_{j,k}^\dagger \hat{a}_{j,k} + g_k(\hat{a}_{j,k}\hat{\sigma}_j^+ + \mathrm{H.c.})]$$

$$g_k = \omega_0 \hat{\mathbf{e}}_k \cdot \mathbf{d}/\sqrt{2\varepsilon_0 \omega_k V}$$

Noisy dynamics in parameter encoding

Master equation:

$$\dot{\rho}(t) = \sum_{j=1}^{n}\{-i\frac{\omega(t)}{2}[\hat{\sigma}_j^+\hat{\sigma}_j^-, \rho(t)] + \frac{\gamma(t)}{2}\check{\mathcal{L}}_j\rho(t)\},$$

$\check{\mathcal{L}}_j\cdot = 2\hat{\sigma}_j^- \cdot \hat{\sigma}_j^+ - \{\cdot, \hat{\sigma}_j^+\hat{\sigma}_j^-\}$, $\gamma(t) + i\omega(t) = -2\frac{\dot{c}(t)}{c(t)}$

$$\dot{c}(t) + i\omega_0 c(t) + \int_0^t f(t-\tau)c(\tau)d\tau = 0$$

under $c(0) = 1$. $f(t-\tau) \equiv \int J(\omega)e^{-i\omega(t-\tau)}d\omega$.
$J(\omega)$: Spectral density, the minimal input of noises

Noisy Q. metrology

$$\delta\omega_0|_{\text{uncor}} = \left\{ \frac{nT[\partial_{\omega_0}\text{Re}(c(t))]^2}{t[1-\text{Re}^2(c(t))]} \right\}^{-1/2}$$

$$\delta\omega_0|_{\text{ent}} = \left\{ \frac{T[\partial_{\omega_0}\text{Re}(c^n(t))]^2}{t[1-\text{Re}^2(c^n(t))]} \right\}^{-1/2}$$

- Ideal limit: $\lim_{g_k\to 0} c(t) = e^{-i\omega_0 t}$, then

$$\delta\omega_0|_{\text{uncor}}^{\text{ideal}} = (nTt)^{-1/2}, \quad \delta\omega_0|_{\text{ent}}^{\text{ideal}} = (n^2 Tt)^{-1/2}$$

- Markovian limit: $c(t) = e^{-[\tilde{\gamma}/2+i(\omega_0+\Delta\omega)]t}$ with $\tilde{\gamma} = 2\pi J(\omega_0)$ and $\Delta\omega = \mathcal{P}\int \frac{J(\omega)}{\omega-\omega_0}d\omega$

$$\min(\delta\omega_0|_{\text{uncor}}) = \min(\delta\omega_0|_{\text{ent}}) = (nT/\tilde{\gamma}e)^{-1/2}$$

Analysis via Laplace transform

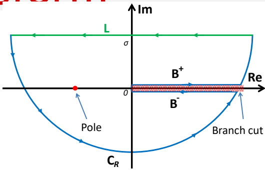

$$
\begin{aligned}
c(t) &= \mathcal{L}^{-1}[\frac{1}{s+i\omega_0+\tilde{K}(s)}] \\
&= Ze^{-iE_{\rm b}t} + \int_{i\sigma+0}^{i\sigma+\infty}\frac{dE}{2\pi}\tilde{\alpha}(-iE)e^{-iEt}
\end{aligned}
$$

where $Z = [1+\int_0^\infty \frac{J(\omega)}{(\varpi_{\rm b}-\omega)^2}d\omega]^{-1}$ and $E_{\rm b}$ is a pole

$$
y(E) \equiv \omega_0 - \int_0^\infty \frac{J(\omega)}{\omega - E}d\omega = E,\ (E = is)
$$

One can prove

$$
\lim_{t\to\infty} c(t) = \begin{cases} 0, & y(0) > 0 \\ Ze^{-iE_0 t}, & y(0) < 0 \end{cases} \tag{1}
$$

Exact long-time metrology precision

Thus when $y(0) < 0$

$$\min(\lim_{t\to\infty} \delta\omega_0|_{\mathrm{ent}}) \leq Z^{-(n+1)} \delta\omega_0|_{\mathrm{ent}}^{\mathrm{ideal}} \tag{2}$$

- The scaling is HL modulated by $Z^{-(n+1)}$ in amplitude

Contents

What is E_b

- The eigenstate of atom-env system:
  $|\varphi_1\rangle = c_0 |+, \{0_k\}\rangle + \sum_k c_k |-, 1_k\rangle$

$$\left.\begin{aligned} \omega_0 c_0 + \sum_k g_k c_k &= E c_0 \\ g_k^* c_0 + \omega_k c_k &= E c_k \end{aligned}\right\} \Rightarrow y(E) \equiv \omega_0 - \int_0^\infty \frac{J(\omega)}{\omega - E} d\omega = E$$

Tong, An, Luo, Oh, PRA 81, 052330 (2010)

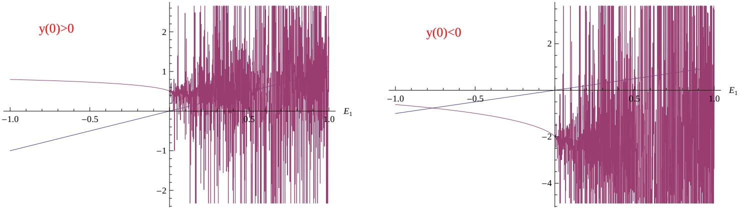

- The pole is just the eigenenergy of the whole system
- We call the isolated eigenstate **bound state**

Contents

A photonic bandgap env formed in circuit QED

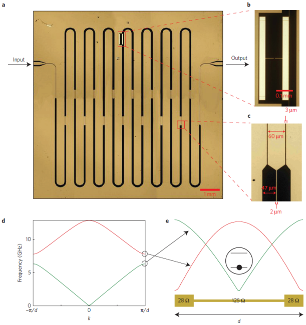

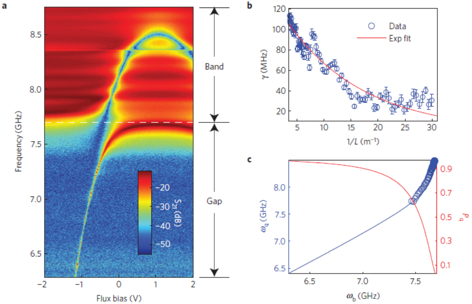

$\omega_c \simeq 8.0$ GHz, $\gamma_0 \simeq 50$ MHz, $\omega_0 \simeq 6.0 \sim 8.5$ GHz

Y. Liu, A. A. Houck, Nat. Phys. 13, 48 (2017)

Population trapping in structured env

Dispersion relation: $\omega_k = \omega_c + A(k - k_0)^2$ with $k_0 = \frac{\omega_c}{c}$

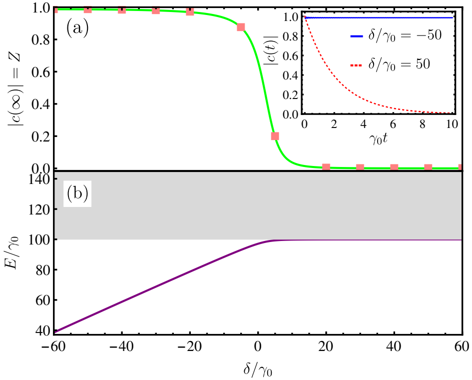

$\delta = \omega_0 - \omega_c$ and $\gamma_0 = \omega_0^3 d^2/(3\pi\epsilon_0 c^3)$. $\omega_c = 100\gamma_0$ is been used.

The regime where the population is trapped matches with the one where a bound state is formed

Metrology precision

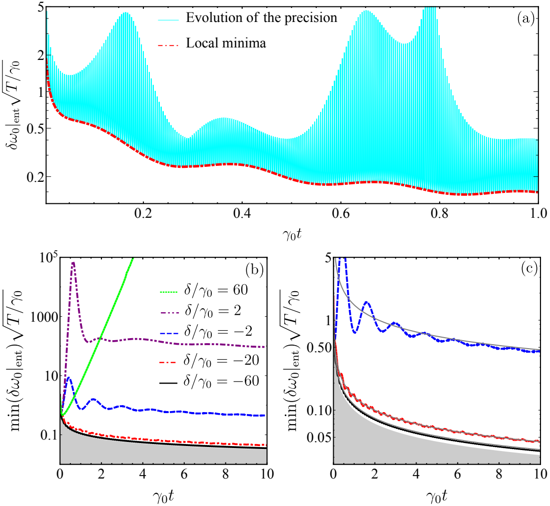

$n = 10$ is been used. Grey area: HL

The HL is restored asymptotically with decreasing δ

Scaling relation in long-time dynamics

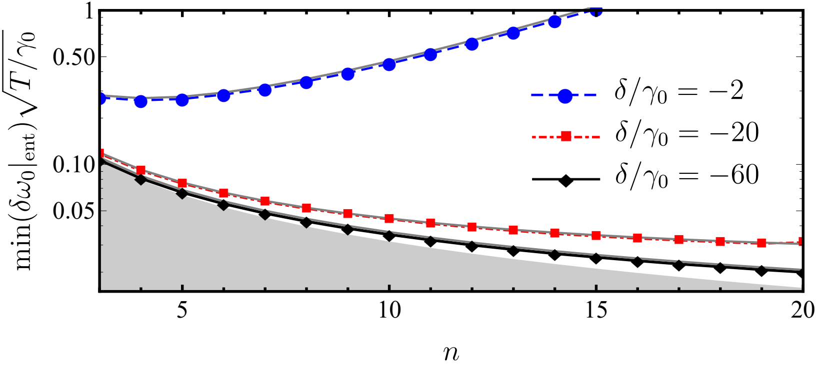

$t = 10/\gamma_0$ is been used. Grey area: HL. Grey curves show the scaling obtained from $Z^{-(n+1)}\delta\omega_0|_{\mathrm{ent}}^{\mathrm{ideal}}$

The precision scaling as $Z^{-(n+1)}\delta\omega_0|_{\mathrm{ent}}^{\mathrm{ideal}}$ in long-time dynamics tends to the HL

Contents

Contents

Ideal case

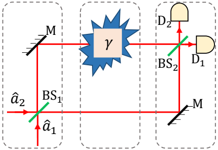

To estimate a parameter γ of a system, we choose two-mode light in $|\psi_{\text{in}}\rangle$ and let it interact with the system to encode the parameter. After the light goes through the MZI, the photon-number difference of the two output ports is measured.

- Input: $|\psi_{\text{in}}\rangle = |\alpha, \xi\rangle$ ($\alpha = |\alpha|e^{i\varphi}$, $\xi = re^{i\phi}$)
- Encode: $\hat{U} = e^{-i\hat{H}_0 t}$ with $\hat{H}_0 = \omega_0 \hat{a}_1^\dagger \hat{a}_1 + (\omega_0 + \gamma)\hat{a}_2^\dagger \hat{a}_2$.

$$|\psi_{\text{out}}\rangle = \hat{V}\hat{U}\hat{V}|\psi_{\text{in}}\rangle, \;\; \hat{V} = e^{i\frac{\pi}{4}(\hat{a}_1^\dagger \hat{a}_2 + \hat{a}_2^\dagger \hat{a}_1)}$$

- Measure $\hat{M} = \hat{a}_1^\dagger \hat{a}_1 - \hat{a}_2^\dagger \hat{a}_2$ ($\delta\gamma = \frac{\delta M}{|d\bar{M}/d\gamma|}$)

$$\min \delta\gamma|_{\gamma t = \frac{\pi}{2}, \phi = 2\varphi} = \frac{(|\alpha|^2 e^{-2r} + \sinh^2 r)^{\frac{1}{2}}}{t(\sinh^2 r - |\alpha^2|)} \simeq \frac{1}{N^{\frac{3}{4}} t}, \;\; \text{(ZL)}$$

R. Demkowicz-Dobrzański, M. Jarzyna, and J. Kołodyński, Progress in Optics 60, 345 (2015)

Contents

Noisy case

Noise presents in encoding step. Then

$$\hat{H} = \hat{H}_0 + \sum_k [\omega_k \hat{b}_k^\dagger \hat{b}_k + g_k(\hat{b}_k^\dagger \hat{a}_2 + \text{h.c.})]$$

The decoherence is governed by **JHA**, Zhang, PRA 76, 042127 (2007)

$$\dot{\rho}(t) = -i[\omega_0 \hat{a}_1^\dagger \hat{a}_1 + \Omega(t)\hat{a}_2^\dagger \hat{a}_2, \rho(t)] + \kappa(t)\check{\mathcal{L}}_{\hat{a}_2}\rho(t)$$

with $\kappa(t) + i\Omega(t) = \dot{c}(t)/c(t)$ and

$$\dot{c}(t) + i(\omega_0 + \gamma)c(t) + \int_0^t f(t-\tau)c(\tau)d\tau = 0$$

with $c(0) = 1$, $f(t-\tau) = \int_0^\infty J(\omega)e^{-i\omega(t-\tau)}d\omega$

Metrology precision

$$
\begin{aligned}
\bar{M} &= \mathrm{Re}[e^{i\omega_0 t}c(t)](\sinh^2 r - |\alpha|^2), \\
\delta M &= \{[\mathrm{Im}(e^{i\omega_0 t}c(t))]^2[|\alpha\cosh r - \alpha^* e^{i\phi}\sinh r|^2 + \sinh^2 r] \\
&\quad +[\mathrm{Re}(e^{i\omega_0 t}c(t))]^2[|\alpha|^2 + \frac{\sinh^2 2r}{2}] + \frac{1-|c(t)|^2}{2} \\
&\quad \times(|\alpha|^2 + \sinh^2 r)\}^{\frac{1}{2}}
\end{aligned}
$$

In the presence of the bound state, $\lim_{t\to\infty} c(t) = Ze^{-iE_0 t}$

$$
\min \delta\gamma|_{\beta=(2\sqrt{N})^{-1}} = \frac{(tN^{3/4})^{-1}}{Z}\left[1 + \frac{1-Z^2}{2Z^2}N^{\frac{1}{2}}\right]^{\frac{1}{2}}
$$

Numerical results

Condition to form the bound state for Ohmic spectrum $J(\omega) = \eta\omega e^{-\omega/\omega_c}$: $\omega_0 + \gamma - \eta\omega_c < 0$

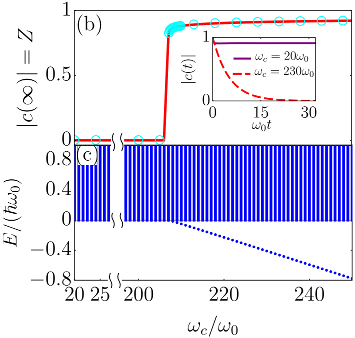

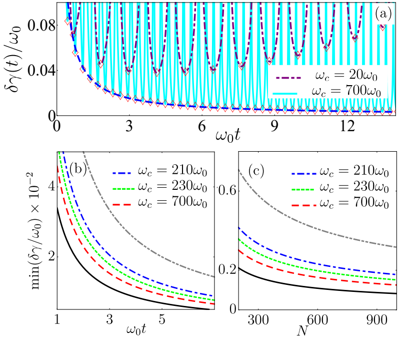

(b): $\eta = 0.02$. (c): $\omega_c = 200\omega_0$. Other parameters are: $\bar{N} = 10^4$ and $\gamma = \pi\omega_0$. Gray line is SQL. Black line is ZL.

Contents

Conclusions

- We have studied the effect of the local dissipative noises on Q. metrology schemes
  1. Ramsey spectroscopy
  2. Mach-Zehnder interferometer
- It is revealed that the precision in the ideal case is asymptotically recoverable in long encoding-time condition
- It is due to the formation of a bound state between each system and its Q. noise
- The result could be generalized readily to other estimation scenarios.

References

1. Y.-S. Wang, C. Chen, **JHA**, New J. Phys. 19, 113019 (2017).
2. K. Bai Z. Peng, H.-G. Luo and **JHA**, *Retrieving ideal precision in noisy quantum optical metrology*, arXiv:1901.06858.

谢谢！